Neural Network-based Robust Anti-sway Control of an Industrial Crane Subjected to Hoisting Dynamics and Uncertain Hydrodynamic Forces

Gyoung-Hahn Kim, Phuong-Tung Pham, Quang Hieu Ngo, and Quoc Chi Nguyen* ⓘD

Abstract: In this paper, a neural network-based robust anti-sway control is proposed for a crane system transporting an underwater object. A dynamic model of the crane system is developed by incorporating hoisting dynamics, hydrodynamic forces, and external disturbances. Considering the various uncertain factors that interfere with accurate payload positioning in water, neural networks are designed to compensate for unknown parameters and unmodeled dynamics in the formulated problem. The neural network-based estimators are embedded in the anti-sway control algorithm, which improves the control performance against uncertainties. A sliding mode control with an exponential reaching law is developed to suppress the sway motions during underwater transportation. The asymptotic stability of the sliding manifold is proved via Lyapunov analysis. The embedded estimator prevents the conservative gain selection of the sliding mode control, thus reducing the chattering phenomena. Simulation results are provided to verify the effectiveness and robustness of the proposed control method.

Keywords: Anti-sway control, crane control, neural network estimator, sliding mode control, underwater transference.

1. INTRODUCTION

Over the past several decades, industrial cranes have been utilized to accomplish various jobs at a variety of locations, including container terminals, warehouses, and construction sites. Recently, beyond such demands confined to land, the necessity to transport underwater objects has emerged due to advanced engineering facilities such as transporting fuel rods in nuclear power plants [1–3, 13], investigating underwater caves, transporting objects from the seabed, etc. However, as the task environment becomes harsh, the control problem of efficient transportation inevitably becomes more challenging because of the existence of more diverse and uncertain factors that interfere with accurate payload positioning. Hence, to maximize the productivity of the crane system operating for objects in water, a novel methodology is required to effectively suppress unexpected payload swing under unfavorable effects such as hydrodynamic forces and unknown flow disturbances.

For crane systems transporting a payload in air, several relevant studies analyzing various industrial cranes, such as gantry cranes, boom cranes, tower cranes, and container cranes, have been conducted. In particular, the control problem of crane systems has primarily focused on methods that effectively suppress unwanted payload swing during transportation. To address this issue, several effective control strategies have been developed for different structures and dynamics. These strategies can be categorized into open-loop control methods [1–7] and closed-loop control methods [8–26]. In particular, the well-developed open-loop control methods are input shaping-based approaches [1–5], which achieve simultaneous positioning control and swing elimination using linearized dynamics. In addition, the method of anti-swing trajectory generation [6,7] is recommended to suppress cargo swinging. Although these open-loop controllers are convenient to implement in practical systems, most of them are sensitive to parametric uncertainties. In contrast, feedback controllers have been developed to enhance the robustness of the control system while ensuring satisfactory performance in swing elimination. Several types of modern control meth-

Gyoung-Hahn Kim and Phuong-Tung Pham are with the School of Mechanical Engineering, Pusan National University, Busan 46241, Korea (e-mails: hahn@pusan.ac.kr; pptung@pusan.ac.kr). Quang Hieu Ngo is with the Department of Mechanical Engineering, Can Tho University, Vietnam (e-mail: nqhieu@ctu.edu.vn). Quoc Chi Nguyen is with the Mechatronics Department, Ho Chi Minh City University of Technology (HCMUT)-Vietnam National University Ho Chi Minh City, 268 Ly Thuong Kiet Street, District 10, Ho Chi Minh City, Vietnam and the Faculty of Electrical Engineering-Electronics-Mechanics-Construction, Dong Nai Technology University, Vietnam (e-mail: nqchi@hcmut.edu.vn).
* Corresponding author.

ods, such as delayed feedback control [8], adaptive nonlinear control [9–12], boundary control [13, 14], sliding mode control [15–23], and intelligent control [24–26] are included in this category.

Although the aforementioned methods for crane systems are effective, their direct application to the control problem of transporting underwater objects is inadvisable due to the complex sway motions, which are distinct from the dynamic behavior in air. When a crane system undertakes object transportation in water, the viscous-induced force (i.e., drag induced force) dampens the payload swing by generating quadratic damping forces, and the additional inertial resistance resulting from the accelerated fluid around the payload provides the added mass (i.e., the extra bulk). Moreover, these hydrodynamic forces primarily include significant uncertainties stemming from the complex underwater environment, making the dynamic behavior more unpredictable. Therefore, to guarantee high productivity of the crane system, the complex sway motions interacting with the hydrodynamic forces should be carefully considered for controller development. At present, only a few works on the control of crane systems under the influence of hydrodynamic forces have been presented in the literature [2, 3, 13]. Notably, the existing works discussed only the position and vibration control of crane systems under extremely relaxed conditions by assuming that i) accurate information of the system parameters and hydrodynamic forces is available and ii) the effects on the hoisting dynamics and external disturbances are negligible. More specifically, in [2], Shah and Hong developed a model of an overhead crane that is utilized to transport a rigid rod in water, and the typical input shaping controller was designed based on a linearized model. Their results were then extended to the vibration control problem of a flexible rod in [3]. A boundary control law was recently proposed to suppress the vortex-induced vibrations of a flexible rod in [13].

Based on the abovementioned results for crane systems transporting underwater objects, it is not difficult to find that many important issues remain open and need to be further investigated with robust control methods. Therefore, in this paper, a neural network-based robust anti-sway control strategy is proposed to address the control problem of how to effectively suppress sway motions subjected to hoisting dynamics and uncertain hydrodynamic forces. The main contributions of this study are as follows.

1) A dynamic model of a crane system under hydrodynamic forces is developed by incorporating hoisting dynamics. Unlike the existing model (which lacks hoisting dynamics), the developed model can enhance the crane system's productivity owing to the simultaneous hoisting operation during trolley traveling motion.

2) To the best of our knowledge, the proposed control method is the first to address the anti-sway control of a crane under uncertain hydrodynamic forces and hoist-

ing dynamics. A neural network-based function estimator is proposed in the control formulation, enabling the effective estimation of unknown parameters in the system, such as hydrodynamic forces. Although the estimator does not directly estimate each parameter, it can evaluate key functions comprising unknown parameters and unmodeled dynamics. Accordingly, the conservative selection of the control gain in the sliding mode control (SMC) can be avoided, thus reducing the chattering phenomena in the control input. Simulation results are also provided to validate the effectiveness of the proposed scheme. Therein, the robustness of the developed controller against the parameter uncertainties of the hydrodynamic forces and external disturbances by water flow is investigated.

The rest of this paper is arranged as follows: In the following section, crane dynamics incorporating the hoisting dynamics and hydrodynamics are introduced, and the control problem is formulated. Then, Section 3 presents the controller design and provides the stability analysis. In Section 4, the simulation results are presented to validate the efficiency of the proposed method. Finally, the conclusions are drawn in Section 5.

2. PROBLEM FORMULATION

A schematic illustration of a 2D crane transporting an underwater object is shown in Fig. 1, where X_o-O_o-Z_o represents the inertial coordinate frame. The corresponding system parameters are described in Table 1. Before deriving the equations of motion, it is assumed that i) the rope is a massless rigid rod, ii) the payload swing exhibits pendulum motion in water, and iii) the payload swing occurs only in the X-Z plane, incorporating the one-directional movement of the trolley. Based on the above assumptions, a 3-degree-of-freedom (3-DOF) crane model is developed as follows:
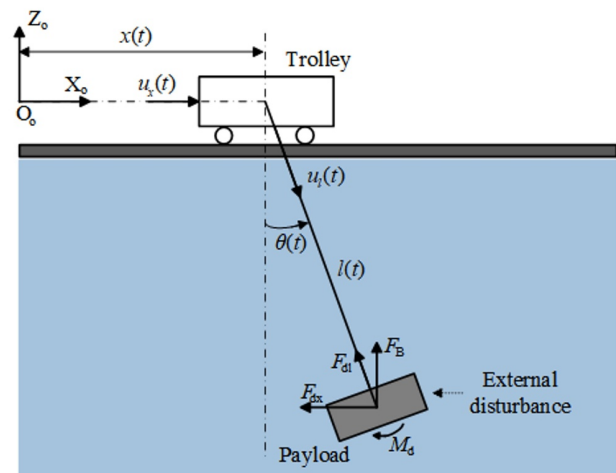

Fig. 1. Schematic illustration of an industrial crane transporting an underwater object.

Table 1. Parameters and variables.

Symbol	Description
m_t, m_p	Trolley and payload masses
I	Mass moment of inertia of the payload
x	Displacement of the trolley
l	Hoist rope length
θ	Sway angle of the payload
F_B	Buoyancy force
F_{dx}, F_{dl}, M_d	Viscous-induced forces and moment with respect to the x-, l-, and θ-directions
m_{rx}, m_{rl}, I_r	Coefficients of additional inertial resistances with respect to the x-, l-, and θ-directions
u_x, u_l	Control forces for the trolley and hoist

2.1. Hydrodynamic forces

Unlike a crane system transporting a payload in the air, the considered crane system's primary concern is the hydrodynamic effects exerted on the payload. In this study, a hydrodynamic model based on the viscous-induced force/moment and an additional inertial resistance (i.e., the added mass/mass moment of inertia) is adopted to account for the hydrodynamic interactions with the object. For engineering purposes, the hydrodynamic model, in its simplified form, is given as follows:

$$\begin{bmatrix} \Sigma_x \\ \Sigma_l \\ \Sigma_\theta \end{bmatrix} = \underbrace{\begin{bmatrix} m_{rx}\dot{v}_x \\ m_{rl}\dot{v}_l \\ I_r\ddot{\theta} \end{bmatrix}}_{\substack{\text{Additional} \\ \text{inertial} \\ \text{resistance} \\ (F_r, M_r)}} + \underbrace{\begin{bmatrix} \frac{1}{2}\rho_w A_{px} v_x |v_x| C_{dx} \\ \left(\frac{1}{2} v_l |v_l| + gl\cos\theta\right)\rho_w A_{pl} C_{dl} \\ \frac{1}{2}\rho_w A_{p\theta} v_\theta |v_\theta| l C_{d\theta} \end{bmatrix}}_{\text{Drag force and drag-induced moment } (F_d, M_d)},$$

(1)

where ρ_w denotes the density of water; m_{rx}, m_{rl}, and I_r are the coefficients of the additional inertial resistance by water; C_{dx}, C_{dl}, and $C_{d\theta}$ are the drag coefficients; A_{px}, A_{pl}, and $A_{p\theta}$ indicate the projected area of the payload corresponding to the x-, l-, and θ-directions, respectively; and v_x, v_l, and v_θ are the velocities of the trolley, rope, and payload, respectively, which are expressed as $v_x = \dot{x}$, $v_l = \dot{l}$, and $v_\theta = \dot{l}\theta + l\dot{\theta}$.

2.2. Dynamic modeling

To obtain the equations of motion, the kinetic energy (K) of the trolley and payload and the potential energy (V) of the payload, respectively, are obtained as follows:

$$K = \frac{1}{2}\left[(m_t + m_p)\dot{x}^2 + (m_p + m_h)\dot{l}^2 + m_p l^2 \dot{\theta}^2 + I\dot{\theta}^2\right]$$
$$\quad + m_p \dot{x}(l\cos\theta\dot{\theta} + \dot{l}\sin\theta),$$
$$V = -(m_p g - \rho_w g V_s)l\cos\theta,$$

(2)

where m_h is the equivalent mass of the hoist mechanism and V_s denotes the submerged volume of the payload. Note

that the buoyancy force $F_B = \rho_w g V_s$ is included in the potential energy (V) as a conservative force. Additionally, the Rayleigh dissipative function is introduced to account for the linear viscous damping in the system and is expressed as follows:

$$D = \frac{1}{2}(\mu_x \dot{x}^2 + \mu_l \dot{l}^2 + \mu_\theta \dot{\theta}^2),$$

(3)

where μ_x, μ_l, and μ_θ are the linear viscous damping coefficients. Then, we utilize Lagrange's equation for the state variables (i.e., the generalized coordinates) $\mathbf{q} = [x, l, \theta]^T$ by considering the hydrodynamic forces in (1) as nonconservative generalized forces. After a series of calculations, the equations of motion for the 3-DOF crane transporting a payload subjected to hydrodynamic forces are derived.

$$(m_t + m_p + m_{rx})\ddot{x} + m_p \sin\theta \ddot{l} + m_p l\cos\theta \ddot{\theta} + \mu_x \dot{x}$$
$$+ 2m_p \cos\theta \dot{l}\dot{\theta} - m_p l\sin\theta\dot{\theta}^2 + \frac{1}{2}\rho_w A_{px} v_x |v_x| C_{dx} = u_x,$$
$$m_p \sin\theta \ddot{x} + (m_p + m_h + m_{rl})\ddot{l} + \mu_l \dot{l} - (m_p g - \rho_w g V_s)\cos\theta$$
$$- m_p l\dot{\theta}^2 + \left(\frac{1}{2} v_l |v_l| + gl\cos\theta\right)\rho_w A_{pl} C_{dl} = u_l,$$
$$m_p l\cos\theta \ddot{x} + (m_p l^2 + I + I_r)\ddot{\theta} + \mu_\theta \dot{\theta} + 2m_p l\dot{l}\dot{\theta}$$
$$+ (m_p g - \rho_w g V_s)l\sin\theta + \frac{1}{2}\rho_w A_{p\theta} v_\theta |v_\theta| l C_{d\theta} = 0.$$

(4)

Equation (4) can be rewritten in a compact matrix-vector form as follows:

$$\mathbf{M}(\mathbf{q})\ddot{\mathbf{q}} + \mathbf{N}(\mathbf{q}, \dot{\mathbf{q}}) = \mathbf{u} + \boldsymbol{\Delta},$$

(5)

where $\mathbf{M}(\mathbf{q}) \in \mathbb{R}^{3\times3}$ denotes the inertia matrix, $\mathbf{N}(\mathbf{q}, \dot{\mathbf{q}}) \in \mathbb{R}^{3\times1}$ represents the composite vector comprising the Coriolis-centripetal term, gravity, linear viscous damping, and the hydrodynamic force, and $\mathbf{u} \in \mathbb{R}^{3\times1}$ is the control input vector. The variable $\boldsymbol{\Delta} \in \mathbb{R}^{3\times1}$ represents the lumped uncertainty vector with a bound given by $\|\boldsymbol{\Delta}\| \leq \boldsymbol{\Delta}_{max}$. The detailed expressions of $\mathbf{M}(\mathbf{q})$, $\mathbf{N}(\mathbf{q}, \dot{\mathbf{q}})$, $\mathbf{u}$, and $\boldsymbol{\Delta}$ are provided as follows:

$$\mathbf{M}(\mathbf{q}) = \begin{bmatrix} m_{11} & m_{12} & m_{13} \\ m_{21} & m_{22} & 0 \\ m_{31} & 0 & m_{33} \end{bmatrix}, \quad \mathbf{N}(\mathbf{q}, \dot{\mathbf{q}}) = \begin{bmatrix} N_1 & N_2 & N_3 \end{bmatrix}^T,$$

$$\mathbf{u} = \begin{bmatrix} u_x & u_l & 0 \end{bmatrix}^T, \quad \boldsymbol{\Delta} = \begin{bmatrix} \Delta_x & \Delta_l & \Delta_\theta \end{bmatrix}^T,$$

where

$$m_{11} = m_t + m_p + m_{rx}, \quad m_{12} = m_p \sin\theta, \quad m_{13} = m_p l\cos\theta,$$
$$m_{21} = m_p \sin\theta, \quad m_{22} = m_p + m_h + m_{rl},$$
$$m_{31} = m_p l\cos\theta, \quad m_{33} = m_p l^2 + I + I_r,$$
$$N_1 = \mu_x \dot{x} + 2m_p \cos\theta \dot{l}\dot{\theta} - m_p l\sin\theta\dot{\theta}^2$$
$$\quad + \frac{1}{2}\rho_w A_{px} v_x |v_x| C_{dx},$$

$$N_2 = \mu_l \dot{l} - m_{\mathrm{p}} l \dot{\theta}^2 - (m_{\mathrm{p}} g - \rho_{\mathrm{w}} g V_{\mathrm{s}}) \cos\theta$$
$$\qquad + \left(\frac{1}{2} v_l |v_l| + gl\cos\theta \right) \rho_{\mathrm{w}} A_{\mathrm{pl}} C_{\mathrm{dl}},$$
$$N_3 = \mu_\theta \dot{\theta} + 2 m_{\mathrm{p}} l \dot{l} \dot{\theta} + (m_{\mathrm{p}} g - \rho_{\mathrm{w}} g V_{\mathrm{s}}) l \sin\theta$$
$$\qquad + \frac{1}{2} \rho_{\mathrm{w}} A_{\mathrm{p}\theta} v_\theta |v_\theta| l C_{\mathrm{d}\theta}.$$

Remark 1: Along with the linear damping force, the drag force in a quadratic form is included in the dynamic model. Furthermore, the total viscous force/moment comprising both the dynamic pressure and hydrostatic pressure contribution is considered in hoisting dynamics to account for the cavity-drag force by the air entrainment behind the payload [27].

Remark 2: Considering that the fluid in the vicinity of the submerged payload is suddenly accelerated by the payload motions, the fluid accelerated by the object, as well as the object itself, must be considered. Therefore, the added mass and inertia are included along with the viscous-induced force and moment, which represent the additional inertia resistance resulting from the accelerated fluid [28].

Remark 3: Unknown instability factors, such as external disturbances and unmodeled dynamics (i.e., the lumped uncertainty vector in the dynamic model), are a challenging issue to be compensated for in the controller design. Moreover, the parameter uncertainty in hydrodynamic forces (i.e., viscous-induced force and additional inertia resistance) is another important issue, which further complicates the control problem by increasing the system's complexities. Hence, a sliding mode-based robust anti-sway control method with the combination of a neural network-based function estimator is developed, which is a distinct aspect from the existing works [2,3,13], in which the effects on the uncertain factors were not properly discussed.

3. MAIN RESULT

To facilitate the control law design, the dynamic equations in (5) can be rearranged in the form of actuated coordinates $\mathbf{q_a} = [x \quad l]^{\mathrm{T}}$ and unactuated coordinates $q_{\mathrm{u}} = \theta$.

$$\ddot{\mathbf{q}}_{\mathbf{a}} = \begin{bmatrix} m_{11} - \dfrac{m_{13}m_{31}}{m_{33}} & m_{12} \\ m_{21} & m_{22} \end{bmatrix}^{-1} \begin{bmatrix} -N_1 + \dfrac{m_{13}N_3}{m_{33}} \\ -N_2 \end{bmatrix}$$
$$+ \begin{bmatrix} m_{11} - \dfrac{m_{13}m_{31}}{m_{33}} & m_{12} \\ m_{21} & m_{22} \end{bmatrix}^{-1} \begin{bmatrix} \Delta_x - \dfrac{m_{13}\Delta_\theta}{m_{33}} \\ \Delta_l \end{bmatrix}$$
$$+ \begin{bmatrix} m_{11} - \dfrac{m_{13}m_{31}}{m_{33}} & m_{12} \\ m_{21} & m_{22} \end{bmatrix}^{-1} \begin{bmatrix} u_x \\ u_l \end{bmatrix}$$
$$= \bar{\mathbf{N}}_{\mathbf{a}} + \bar{\boldsymbol{\Delta}}_{\mathbf{a}} + \bar{\mathbf{M}}_{\mathbf{a}} \mathbf{u}_{\mathbf{a}},$$

$$\ddot{q}_{\mathrm{u}} = \left(\begin{bmatrix} -\dfrac{m_{31}}{m_{33}} \\ 0 \end{bmatrix}^{\mathrm{T}} \bar{\mathbf{N}}_{\mathbf{a}} - \dfrac{N_3}{m_{33}} \right)$$
$$+ \left(\begin{bmatrix} -\dfrac{m_{31}}{m_{33}} \\ 0 \end{bmatrix}^{\mathrm{T}} \bar{\boldsymbol{\Delta}}_{\mathbf{a}} + \dfrac{\Delta_\theta}{m_{33}} \right) + \begin{bmatrix} -\dfrac{m_{31}}{m_{33}} \\ 0 \end{bmatrix}^{\mathrm{T}} \bar{\mathbf{M}}_{\mathbf{a}} \mathbf{u}_{\mathbf{a}}$$
$$= \bar{N}_{\mathrm{u}} + \bar{\Delta}_{\mathrm{u}} + \bar{M}_{\mathrm{u}} \mathbf{u}_{\mathbf{a}}. \tag{6}$$

Considering that the control objective is to transport a payload to the desired target position $\mathbf{q_a^d} = [x_{\mathrm{d}} \quad l_{\mathrm{d}}]^{\mathrm{T}}$ with zero swing (i.e., $q_{\mathrm{u}}^{\mathrm{d}} = 0$), the error dynamics are obtained as follows:

$$\ddot{\mathbf{e}}_{\mathbf{a}} = \bar{\mathbf{N}}_{\mathbf{a}} + \bar{\boldsymbol{\Delta}}_{\mathbf{a}} + \bar{\mathbf{M}}_{\mathbf{a}} \mathbf{u}_{\mathbf{a}},$$
$$\ddot{e}_{\mathrm{u}} = \bar{N}_{\mathrm{u}} + \bar{\Delta}_{\mathrm{u}} + \bar{M}_{\mathrm{u}} \mathbf{u}_{\mathbf{a}}. \tag{7}$$

In the above equations, it is noted that the control input vector $\mathbf{u}_{\mathbf{a}}$ appears in both the actuated and unactuated dynamics due to the underactuated property of the crane system. This implies that the cargo swing should be indirectly controlled through the coupling effect with the actuated dynamics. In this study, to stabilize the error states $e \in \mathbb{R}^3$ with fewer control inputs $\mathbf{u}_{\mathbf{a}} \in \mathbb{R}^2$, the following sliding manifold $\boldsymbol{\sigma} = [\sigma_1, \sigma_2]^{\mathrm{T}}$ is designed.

$$\boldsymbol{\sigma} = \dot{\mathbf{e}}_{\mathbf{a}} + \boldsymbol{\alpha} \mathbf{e}_{\mathbf{a}} + \boldsymbol{\beta} \dot{e}_{\mathrm{u}} + \gamma e_{\mathrm{u}}, \tag{8}$$

where $\boldsymbol{\alpha} = \mathrm{diag}(\alpha_1, \alpha_2)$, $\boldsymbol{\beta} = [\beta_1, 0]^{\mathrm{T}}$, and $\gamma = [\gamma_1, 0]^{\mathrm{T}}$ indicate positive gains. Then, the sliding dynamics are derived as follows:

$$\dot{\boldsymbol{\sigma}} = \left[\bar{\mathbf{N}}_{\mathbf{a}} + \boldsymbol{\alpha} \dot{\mathbf{e}}_{\mathbf{a}} + \boldsymbol{\beta} \bar{N}_{\mathrm{u}} + \gamma \dot{e}_{\mathrm{u}} \right] + \left[\bar{\boldsymbol{\Delta}}_a + \boldsymbol{\beta} \bar{\Delta}_{\mathrm{u}} \right]$$
$$\qquad + \left[\bar{\mathbf{M}}_{\mathbf{a}} + \boldsymbol{\beta} \bar{\mathbf{M}}_{\mathbf{u}} \right] \mathbf{u}_{\mathbf{a}}$$
$$= \boldsymbol{\Psi} + \left[\bar{\boldsymbol{\Delta}}_{\mathbf{a}} + \boldsymbol{\beta} \bar{\Delta}_{\mathrm{u}} \right] + \left[\bar{\mathbf{M}}_{\mathbf{a}} + \boldsymbol{\beta} \bar{\mathbf{M}}_{\mathbf{u}} \right] \mathbf{u}_{\mathbf{a}}$$
$$= \boldsymbol{\Psi} + \boldsymbol{\Omega}(t, \boldsymbol{\sigma}) + \left[\bar{\mathbf{M}}_{\mathbf{a}} + \boldsymbol{\beta} \bar{\mathbf{M}}_{\mathbf{u}} \right] \mathbf{u}_{\mathbf{a}}, \tag{9}$$

where the unknown uncertainties $\boldsymbol{\Omega}(t, \boldsymbol{\sigma}) = [\Omega_1 \ \Omega_2]^{\mathrm{T}}$ are globally bounded (i.e., $\|\boldsymbol{\Omega}(t, \boldsymbol{\sigma})\| \leq \delta$). Based on the sliding dynamics, the sliding mode control with an exponential reaching law is designed as follows:

$$\mathbf{u}_{\mathbf{a}} = - \left[\bar{\mathbf{M}}_{\mathbf{a}} + \boldsymbol{\beta} \bar{\mathbf{M}}_{\mathbf{u}} \right]^{-1} \left[\boldsymbol{\rho} (\dot{\mathbf{e}}_{\mathbf{a}} + \boldsymbol{\alpha} \mathbf{e}_{\mathbf{a}} + \boldsymbol{\beta} \dot{e}_{\mathrm{u}} + \gamma e_{\mathrm{u}}) \right.$$
$$\left. + \boldsymbol{\Psi} + \mathbf{K} \mathrm{sgn}(\boldsymbol{\sigma}) \right]. \tag{10}$$

Here, $\boldsymbol{\rho} = \mathrm{diag}(\rho_1, \rho_2)$ and $K = \mathrm{diag}(k_1, k_2)$ indicate positive gains. If the parameter information in (9) is entirely accurate, the sliding mode control law in (10) can achieve effective control performance with low chattering and fast convergence speed. However, it is not easy to obtain accurate parameter information and dynamic models in most practical cases, thus it requires the conservative switching control gain that causes chattering phenomena. For the considered system, the uncertain hydrodynamic force in (1) is primarily responsible for the inevitable increase in the system uncertainties. Therefore, to resolve this issue,

a neural network-based adaptive algorithm is designed in this study.

According to the global approximation characteristics [29, 30], neural networks can approximate any function. Regarding the control framework in this study, the vector $\boldsymbol{\Psi} = [\Psi_1 \ \Psi_2]^T \in \mathbb{R}^2$ containing model information such as uncertain hydrodynamic forces is approximated by radial basis function (RBF) networks with n-hidden layers. Then, the neural networks are updated by the Lyapunov-based online estimation algorithm. The mathematical expressions of the proposed scheme are as follows:

$$\Psi_i = \mathbf{W}_i^T \mathbf{h}_i(\mathbf{z}) + \varepsilon_i,$$
$$\dot{\hat{\mathbf{W}}}_i = -\boldsymbol{\Sigma}_i \mathbf{h}_i(\mathbf{z})\sigma_i, \text{ for } i = 1, 2, \quad (11)$$

where $\mathbf{W}_i$, $\hat{\mathbf{W}}_i \in \mathbb{R}^{n \times 1}$ denotes the weighting matrix and the estimated weighting matrix, respectively, ε_i denotes the approximation error which has a significantly small value, and $\boldsymbol{\Sigma}_i = \text{diag}(\lambda_1, \cdots, \lambda_n) \in \mathbb{R}^{n \times n}$ represents the positive adaptation gains. $\mathbf{h}_1(\mathbf{z}) = \mathbf{h}_2(\mathbf{z}) = [h_1, h_2, ..., h_n]$ are the activation functions, where the Gaussian function h_j for the neural net j in the hidden layer is given as follows:

$$h_j = \exp\left(-\frac{\|\mathbf{z} - \mathbf{c}_j\|^2}{2b_j^2}\right), \quad j = 1, ..., n, \quad (12)$$

where $\mathbf{z} = [\mathbf{e}_a^T \ e_u \ \dot{\mathbf{e}}_a^T \ \dot{e}_u]^T \in \mathbb{R}^6$ is the input vector in the input layer, $\mathbf{c}_j \in \mathbb{R}^6$ denotes the design parameter for the center point of the Gaussian function in the neural network, and b_j represents the width value of the Gaussian function that can be properly determined in the design process. After embedding (11) into (10), the adaptive neural network-based sliding mode control law is finally derived as follows:

$$\mathbf{u}_a = -\left[\bar{\mathbf{M}}_a + \boldsymbol{\beta}\bar{\mathbf{M}}_u\right]^{-1}\left[\boldsymbol{\rho}(\dot{\mathbf{e}}_a + \boldsymbol{\alpha}\mathbf{e}_a + \boldsymbol{\beta}\dot{e}_u + \gamma e_u) + \hat{\boldsymbol{\Psi}} + \mathbf{K}\,\text{sgn}(\boldsymbol{\sigma})\right]. \quad (13)$$

Here $\hat{\boldsymbol{\Psi}} = [\hat{\Psi}_1 \ \hat{\Psi}_2]^T$ is obtained from

$$\hat{\Psi}_i = \hat{\mathbf{W}}_i^T \mathbf{h}_i(\mathbf{z}), \text{ for } i = 1, 2. \quad (14)$$

To illustrate the entire control system design process, a block diagram is provided in Fig. 2.

Lemma 1 [20]**:** Suppose that the sliding manifold given in (8) is asymptotically stable as time goes to infinity. Then, the error dynamics are asymptotically stable in the sliding mode as time goes to infinity, which implies that the state errors $\mathbf{e}_a$, $\dot{\mathbf{e}}_a$, e_u, and $\dot{e}_u$ converge to zero.

Theorem 1: Consider the error dynamics (7), the sliding manifold (8), and the sliding dynamics (9). Then, the proposed control law (13) with the neural network-based adaptive algorithm in (11) ensures that the sliding manifold $\boldsymbol{\sigma}$ is asymptotically stable as time goes to infinity.
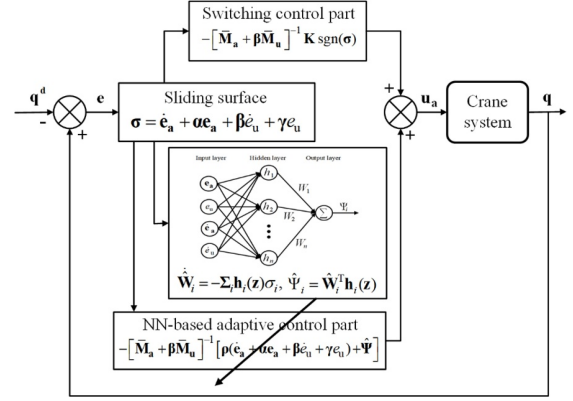

Fig. 2. Structure of control system.

Proof: Let us introduce a nonnegative Lyapunov function candidate in the following form:

$$V = \frac{1}{2}\boldsymbol{\sigma}^T\boldsymbol{\sigma} + \frac{1}{2}\tilde{\mathbf{W}}_1^T\boldsymbol{\Sigma}_1^{-1}\tilde{\mathbf{W}}_1 + \frac{1}{2}\tilde{\mathbf{W}}_2^T\boldsymbol{\Sigma}_2^{-1}\tilde{\mathbf{W}}_2, \quad (15)$$

where $\tilde{\mathbf{W}}_1 = \hat{\mathbf{W}}_1 - \mathbf{W}_1$ and $\tilde{\mathbf{W}}_2 = \hat{\mathbf{W}}_2 - \mathbf{W}_2$. The derivative of the Lyapunov function candidate with respect to time leads to

$$\begin{aligned} \dot{V} =& \boldsymbol{\sigma}^T\dot{\boldsymbol{\sigma}} + \tilde{\mathbf{W}}_1^T\boldsymbol{\Sigma}_1^{-1}\dot{\hat{\mathbf{W}}}_1 + \tilde{\mathbf{W}}_2^T\boldsymbol{\Sigma}_2^{-1}\dot{\hat{\mathbf{W}}}_2 \\ =& \boldsymbol{\sigma}^T\left(\bar{\mathbf{N}}_a + \boldsymbol{\alpha}_1\dot{\mathbf{e}}_a + \boldsymbol{\beta}_1\bar{N}_u + \boldsymbol{\beta}_2 e_u\right) + \boldsymbol{\sigma}^T\left(\bar{\boldsymbol{\Delta}}_a + \boldsymbol{\beta}_1\bar{\Delta}_u\right) \\ & + \boldsymbol{\sigma}^T\left(\bar{\mathbf{M}}_a + \boldsymbol{\beta}_1\bar{\mathbf{M}}_u\right)\mathbf{u}_a + \tilde{\mathbf{W}}_1^T\boldsymbol{\Sigma}_1^{-1}\dot{\hat{\mathbf{W}}}_1 \\ & + \tilde{\mathbf{W}}_2^T\boldsymbol{\Sigma}_2^{-1}\dot{\hat{\mathbf{W}}}_2 \\ =& \boldsymbol{\sigma}^T\left\{\boldsymbol{\Psi} + \left(\bar{\boldsymbol{\Delta}}_a + \boldsymbol{\beta}_1\bar{\Delta}_u\right) + \left(\bar{\mathbf{M}}_a + \boldsymbol{\beta}_1\bar{\mathbf{M}}_u\right)\mathbf{u}_a\right\} \\ & + \tilde{\mathbf{W}}_1^T\boldsymbol{\Sigma}_1^{-1}\dot{\hat{\mathbf{W}}}_1 + \tilde{\mathbf{W}}_2^T\boldsymbol{\Sigma}_2^{-1}\dot{\hat{\mathbf{W}}}_2. \quad (16) \end{aligned}$$

Inserting control law (13) into (16) yields the following:

$$\begin{aligned} \dot{V} =& -\boldsymbol{\sigma}^T\boldsymbol{\rho}\boldsymbol{\sigma} - \boldsymbol{\sigma}^T\left(\mathbf{K}\,\text{sgn}(\boldsymbol{\sigma}) - \boldsymbol{\Omega}(t, \boldsymbol{\sigma})\right) + \boldsymbol{\sigma}^T\tilde{\boldsymbol{\Psi}} \\ & + \tilde{\mathbf{W}}_1^T\boldsymbol{\Sigma}_1^{-1}\dot{\hat{\mathbf{W}}}_1 + \tilde{\mathbf{W}}_2^T\boldsymbol{\Sigma}_2^{-1}\dot{\hat{\mathbf{W}}}_2, \quad (17) \end{aligned}$$

where

$$\tilde{\boldsymbol{\Psi}} = \begin{bmatrix}\tilde{\Psi}_1 & \tilde{\Psi}_2\end{bmatrix}^T \text{ and}$$
$$\tilde{\Psi}_i = \hat{\Psi}_i - \Psi_i = \tilde{\mathbf{W}}_i^T\mathbf{h}_i(\mathbf{z}) - \varepsilon_i, \text{ for } i = 1, 2.$$

From (11) and (17), we have

$$\begin{aligned} \dot{V} =& -\boldsymbol{\sigma}^T\boldsymbol{\rho}\boldsymbol{\sigma} - \boldsymbol{\sigma}^T(\mathbf{K}\,\text{sgn}(\boldsymbol{\sigma}) - \boldsymbol{\Omega}(t, \boldsymbol{\sigma})) + \sigma_1\tilde{\Psi}_1 + \sigma_2\tilde{\Psi}_2 \\ & + \tilde{\mathbf{W}}_1^T\boldsymbol{\Sigma}_1^{-1}\dot{\hat{\mathbf{W}}}_1 + \tilde{\mathbf{W}}_2^T\boldsymbol{\Sigma}_2^{-1}\dot{\hat{\mathbf{W}}}_2 \\ =& -\boldsymbol{\sigma}^T\boldsymbol{\rho}\boldsymbol{\sigma} - \boldsymbol{\sigma}^T(\mathbf{K}\,\text{sgn}(\boldsymbol{\sigma}) - \boldsymbol{\Omega}(t, \boldsymbol{\sigma})) - (\sigma_1\varepsilon_1 + \sigma_2\varepsilon_2) \\ & + \left(\sigma_1\tilde{\mathbf{W}}_1^T\mathbf{h}_1(\mathbf{z}) + \tilde{\mathbf{W}}_1^T\boldsymbol{\Sigma}_1^{-1}\dot{\hat{\mathbf{W}}}_1\right) \\ & + \left(\sigma_2\tilde{\mathbf{W}}_2^T\mathbf{h}_2(\mathbf{z}) + \tilde{\mathbf{W}}_2^T\boldsymbol{\Sigma}_2^{-1}\dot{\hat{\mathbf{W}}}_2\right) \\ =& -\boldsymbol{\sigma}^T\boldsymbol{\rho}\boldsymbol{\sigma} - \boldsymbol{\sigma}^T\left(\mathbf{K}\,\text{sgn}(\boldsymbol{\sigma}) - \boldsymbol{\Omega}(t, \boldsymbol{\sigma}) + \boldsymbol{\varepsilon}\right), \quad (18) \end{aligned}$$

where $\boldsymbol{\varepsilon} = \begin{bmatrix} \varepsilon_1 & \varepsilon_2 \end{bmatrix}^{\mathrm{T}}$ are sufficiently small values that can be omitted for subsequent analysis (see [29]). Thus, $\mathbf{K}$ can be designed such that, $\delta \leq \|\mathbf{K}\,\mathrm{sgn}(\boldsymbol{\sigma})\|$, which implies that $\dot{V} \leq 0$. The above equations indicate that the sliding manifold $\boldsymbol{\sigma}$ and the weighting error matrix $\tilde{\mathbf{W}}$ are apparently bounded. Additionally, $\dot{V}$ is uniformly continuous in time. Therefore, it can be concluded that $\lim_{t\to\infty}\dot{V} = 0$ and $\lim_{t\to\infty}\boldsymbol{\sigma} = 0$ by means of Barbalat's lemma. Then, as long as the occurrence of the sliding mode is ensured, the state error convergence is guaranteed by the application of Lemma 1. □

Remark 4: Regarding the control parameters, some guidelines are provided to facilitate the tuning process in practical applications. For successful neural network-based function estimation, the center vector $\mathbf{c}_j$, which represents the central coordination of the Gaussian function for neural net j is designed within the effective mapping of the Gaussian membership function. This implies that the scope of $\mathbf{c}_j$ should be selected to be wider than the scope of the input to the input layer. Likewise, the width value b_j should be determined such that the scope of the network input $\mathbf{z}$ is sufficient to be covered by the wider Gaussian function. Other parameters (ρ_1, ρ_2, k_1, and k_2) are obtained by trial and error, which is similar to the tuning process of control gains in the traditional SMC.

4. NUMERICAL SIMULATION

In this section, simulation results are presented to verify the effectiveness of the proposed control method. The dynamic model in (5) was simulated for two different cases: i) the normal crane system, and ii) the uncertain crane system. Regarding the uncertain crane system, parameter uncertainties in the payload mass and hydrodynamic forces were considered, and an external disturbance was introduced to account for the unknown hydrodynamic interactions with water.

The system parameters used in the simulation are as follows: $m_t = 5$ kg, $m_p = 0.73$ kg, $m_h = 0.5$ kg, $I = 6.86 \times 10^{-4}$ kg·m^2, $g = 9.81$ m/s^2, $\rho_w = 1000$ kg/m^3, $V_s = 3 \times 10^{-4}$ m^3, $\mu_x = 0.003$, $\mu_l = 0.0001$, $\mu_\theta = 0.03$, $m_{rx} = 2$, $m_{rl} = 2$, $I_r = 5.3 \times 10^{-4}$, $C_{dx} = 0.7$, $C_{dl} = 0.0001$, and $C_{d\theta} = 0.06$. The parameters of the proposed controller are selected as follows: $\alpha_1 = 0.3$, $\alpha_2 = 0.4$, $\beta_1 = -0.01$, $\gamma_1 = -4$, $\rho_1 = 25$, $\rho_2 = 25$, $k_1 = 0.02$, and $k_2 = 0.02$. In this study, an RBF network with 9 hidden layers was designed to estimate the unknown functions, which is given as follows:

$$\mathbf{c} = \begin{bmatrix} -2 & -1.5 & -1 & -0.5 & 0 & 0.5 & 1 & 1.5 & 2 \\ -2 & -1.5 & -1 & -0.5 & 0 & 0.5 & 1 & 1.5 & 2 \\ -2 & -1.5 & -1 & -0.5 & 0 & 0.5 & 1 & 1.5 & 2 \\ -2 & -1.5 & -1 & -0.5 & 0 & 0.5 & 1 & 1.5 & 2 \\ -2 & -1.5 & -1 & -0.5 & 0 & 0.5 & 1 & 1.5 & 2 \\ -2 & -1.5 & -1 & -0.5 & 0 & 0.5 & 1 & 1.5 & 2 \end{bmatrix},$$
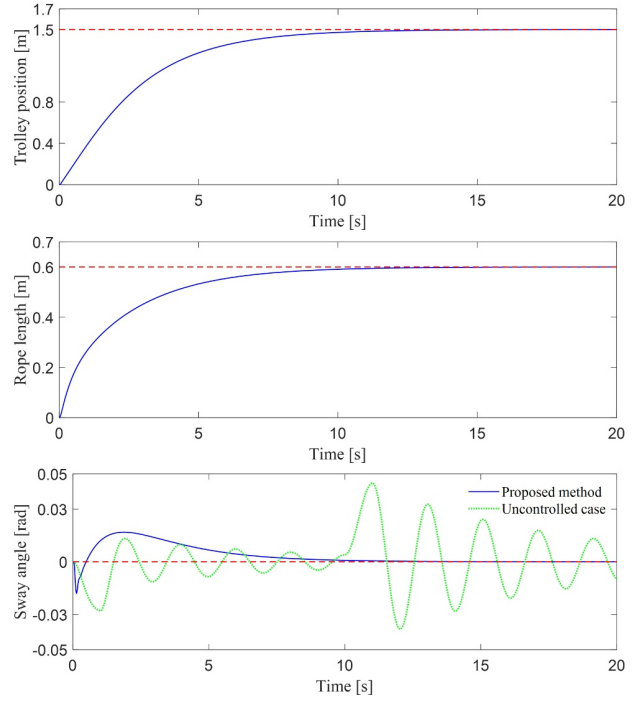
Fig. 3. System responses under hydrodynamic forces.

$$\boldsymbol{\Sigma} = \mathrm{diag}(15, \cdots, 15) \in \mathbb{R}^{9\times 9},$$
$$\mathbf{b} = \begin{bmatrix} 5 & 5 & 5 & 5 & 5 & 5 & 5 & 5 & 5 \end{bmatrix}. \tag{19}$$

Case 1: The first simulation was conducted to verify the control performance of the proposed method by assuming the availability of accurate parameter information. Throughout the simulations, the desired positions of the trolley and rope length were set to 1.5 m and 0.6 m, respectively.

The corresponding simulation results are shown in Fig. 3. Regarding the controlled case, the trolley's excellent tracking performance and the desired rope length were achieved, and the payload swing was remarkably eliminated at the goal position. On the other hand, the uncontrolled case (i.e., the trolley is driven by the trapezoidal velocity profile based on maximum velocity) shows that a complete swing elimination by viscous water damping is more time-consuming than the controlled case. Therefore, these simulation results demonstrate that efficient transportation is guaranteed by the proposed method when the payload is subjected to hydrodynamic forces that interfere with the process of achieving accurate positioning.

Case 2: The second simulation of the proposed control law demonstrated the control performance in a more practical case (i.e., when accurate parameter information is not available). In this simulation, the payload mass was changed from 0.73 kg to 1.2 kg, and the parameters of the hydrodynamic forces were varied to investigate the effects on the uncertain hydrodynamic forces: $\mu_x = 0.001$, $\mu_l =$
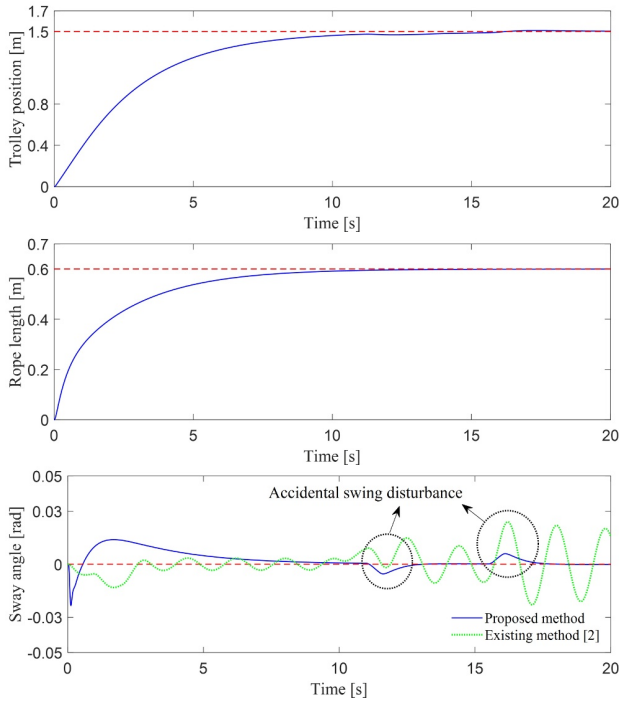
Fig. 4. System responses under unknown parameters, hydrodynamic forces, and external disturbance.

Fig. 5. Neural network-based function estimation.

Fig. 6. Control inputs.

0.001, $\mu_\theta = 0.06$, $C_{dx} = 0.3$, $C_{dl} = 0.001$, and $C_{d\theta} = 0.5$. Additionally, the external swing disturbance acting on the payload was included to account for the effect of the sudden impact by water flow, which is expressed as follows:

$$\Delta_\theta(t) = \begin{cases} -0.05\,\text{N}, & \text{if } 11\text{ s} \le t \le 11.5\text{ s}, \\ 0.05\,\text{N}, & \text{if } 15.5\text{ s} \le t \le 16\text{ s}, \\ 0, & \text{otherwise.} \end{cases} \quad (20)$$

The control performance of the proposed method is compared with a well-tuned input-shaping control scheme in the literature. According to [2], the ZVD shaper for transporting the underwater object can be designed as follows:

$$\begin{bmatrix} A_i \\ t_i \end{bmatrix} = \begin{bmatrix} \frac{1}{1+2K+K^2} & \frac{2K}{1+2K+K^2} & \frac{K^2}{1+2K+K^2} \\ 0 & \frac{\pi}{\omega_d} & \frac{2\pi}{\omega_d} \end{bmatrix}$$
$$= \begin{bmatrix} 0.2654 & 0.4995 & 0.2351 \\ 0 & 0.9660 & 1.9319 \end{bmatrix}, \quad (21)$$

where K and ω_d are calculated as $e^{-\pi\zeta/\sqrt{1-\zeta^2}}$ and $\omega_n\sqrt{1-\zeta^2}$, respectively, using the natural frequency ω_n and damping ratio ζ.

The simulation results of Case 2 are shown in Figs. 4-6. Compared with the proposed method, Fig. 4 demonstrates that the vibration suppression performance of the existing control method is degraded owing to its high sensitivity to parameter uncertainties and external disturbances. However, regarding the proposed method, it can be found that the parameter uncertainties in the payload mass and
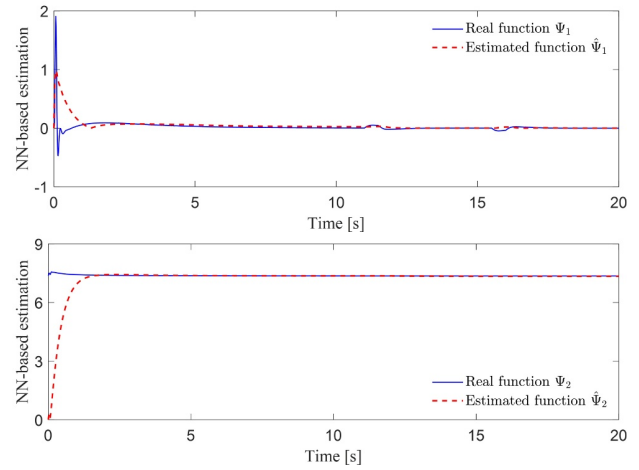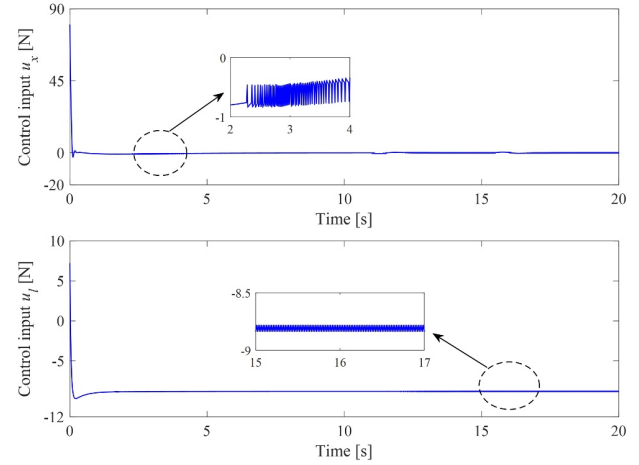
hydrodynamic forces do not significantly influence the payload sway angle and the accuracy of the trolley positioning/payload hoisting. Although exact parameter values were not given as prior information, the proposed neural network-based adaptive algorithm could effectively estimate the unknown function as shown in Fig. 5. The result in the third subpart of Fig. 4 also reveals that the proposed control scheme can suppress and damp out the payload swings in an effective manner in the presence of an accidental swing disturbance (i.e., external disturbance). Finally, as shown in Fig. 6, only small amounts of the chattering phenomena were observed in the control input because the proposed method with the neural network-based function estimator makes it possible to avoid a large switching control gain in the design process. From these results, it can be concluded that the proposed method allows for robustness, which is essential for practical use.

5. CONCLUSION

This study proposes a neural network-based robust anti-sway control method for the control problem of industrial cranes transporting an underwater object. When the payload is subjected to hydrodynamic forces, the control model was developed by incorporating the hoisting dynamics into the payload dynamics. To address the uncertainties in the system parameters and hydrodynamic forces, a neural network-based estimator was successfully designed to estimate the key functions in the control system, which avoids the high control gains required to guarantee robustness. By applying the proposed sliding-mode anti-sway control law, a cargo interacting with the uncertain hydrodynamics can be transported to the desired location, and the effect on the accidental swing disturbance can be effectively suppressed with small control input chattering. The asymptotic stability was proven with the Lyapunov method, without any linearization of the complex nonlinear dynamics. The effectiveness and robustness of the proposed controller were demonstrated through simulations. In future studies, the control problem in the three-dimensional space undertaking underwater transportation will be further analyzed with experimental verification.

REFERENCES

[1] U. H. Shah and K.-S. Hong, *Dynamics and Control of Industrial Cranes*, Springer, ISBN 978-987-13-5769-5, 2019.

[2] U. H. Shah and K.-S. Hong, "Input shaping control of a nuclear power plant's fuel transport system," *Nonlinear Dynamics*, vol. 77, no. 4, pp. 1737-1748, 2014.

[3] U. H. Shah, K.-S. Hong, and S. H. Choi, "Open-loop vibration control of an underwater system: Application to refueling machine," *IEEE-ASME Transactions on Mechatronics*, vol. 22, no. 4, pp. 1622-1632, 2017.

[4] D. Fujioka and W. Singhose, "Optimized input-shaped model reference control on double-pendulum system," *Journal of Dynamic Systems, Measurement, and Control*, vol. 140, no. 10, pp. 101004, 2018.

[5] J. Peng, J. Huang, and W. Singhose, "Payload twisting dynamics and oscillation suppression of tower cranes during slewing motions," *Nonlinear Dynamics*, vol. 98, no. 2, pp. 1041-1048, 2019.

[6] H.-H. Lee, "Motion planning for three-dimensional overhead cranes with high-speed load hoisting," *International Journal of Control*, vol. 78, no. 12, pp. 875-886, 2005.

[7] T. Yang, N. Sun, H. Chen, and Y. C. Fang, "Motion trajectory-based transportation control for 3-D boom cranes: Analysis, design, and experiments," *IEEE Transactions on Industrial Electronics*, vol. 66, no. 5, pp. 3636-3646, 2019.

[8] Z. N. Masoud and A. H. Nayfeh, "Sway reduction on container cranes using delayed feedback controller," *Nonlinear Dynamics*, vol. 34, no. 3, pp. 347-358, 2003.

[9] N. Sun, Y. Fang, H. Chen, and B. He, "Adaptive nonlinear crane control with load hoisting/lowering and unknown parameters: Design and experiments," *IEEE/ASME Transactions on Mechatronics*, vol. 20, no. 5, pp. 2107-2119, 2015.

[10] N. Sun, Y. Fu, T. Yang, J. Zhang, Y. Fang, and X. Xin, "Nonlinear motion control of complicated dual rotary crane systems without velocity feedback: Design, analysis, and hardware experiments," *IEEE Transactions on Automation Science and Engineering*, vol. 17, no. 2, pp. 1017-1029, 2020.

[11] W. Sun, S.-F. Su, J. Xia, and Y. Wu, "Adaptive tracking control of wheeled inverted pendulums with periodic disturbances," *IEEE Transactions on Cybernetics*, vol. 50, no. 5, pp. 1867-1876, 2020.

[12] B.-J. Park, P.-T. Pham, and K.-S. Hong, "Model reference robust adaptive control of control element drive mechanism in a nuclear power plant," *International Journal of Control Automation and Systems*, vol. 18, no. 7, pp. 1651-1661, 2020.

[13] U. H. Shah and K.-S. Hong, "Active vibration control of a flexible rod moving in water: Application to nuclear refueling machines," *Automatica*, vol. 93, pp. 231-243, 2018.

[14] K.-S. Hong and P.-T. Pham, "Control of axially moving systems: A review," *International Journal of Control Automation and Systems*, vol. 17, no. 10, pp. 2610-2623, 2019.

[15] M. H. Zhang, Y. F. Zhang, and X. G. Cheng, "An enhanced coupling PD with sliding mode control method for underactuated double-pendulum overhead crane systems," *International Journal of Control Automation and Systems*, vol. 17, no. 6, pp. 1579-1588, 2019.

[16] A. M. Singh and Q. P. Ha, "Fast terminal sliding control application for second-order underactuated systems," *International Journal of Control Automation and Systems*, vol. 17, no. 8, pp. 1884-1898, 2019.

[17] L. A. Tuan, "Fractional-order fast terminal back-stepping sliding mode control of crawler cranes," *Mechanism and Machine Theory*, vol. 137, pp. 297-314, 2019.

[18] O. Jedda and A. Douik, "Optimal discrete-time integral sliding mode control for piecewise affine systems," *International Journal of Control Automation and Systems*, vol. 17, no. 5, pp. 1221-1232, 2019.

[19] G.-H. Kim, "Continuous integral sliding mode control of an offshore container crane with input saturation," *International Journal of Control Automation and Systems*, vol. 18, no. 9, pp. 2326-2336, 2020.

[20] G.-H. Kim and K.-S. Hong, "Adaptive sliding-mode control of an offshore container crane with unknown disturbances," *IEEE/ASME Transactions on Mechatronics*, vol. 24, no. 6, pp. 2850-2861, 2019.

[21] Q. H. Ngo, N. P. Nguyen, C. N. Nguyen, T. H. Tran, and V. H. Bui, "Payload pendulation and position control systems for an offshore container crane with adaptive-gain sliding mode control," *Asian Journal of Control*, pp. 1-10, 2019. DOI: 10.1002/asjc.2124

[22] L. A. Tuan, H. M. Cuong, P. V. Trieu, L. C. Nho, V. D. Thuan, and L. V. Anh, "Adaptive neural network sliding mode control of shipboard container cranes considering actuator backlash," *Mechanical Systems and Signal Processing*, vol. 112, pp. 233-250, 2018.

[23] M.-S. Park, D. Chwa, and M. Eom, "Adaptive sliding-mode antisway control of uncertain overhead cranes with high-speed hoisting motion," *IEEE Transactions on Fuzzy Systems*, vol. 22, no. 5, pp. 1262-1271, 2014.

[24] W. Sun, S.-F. Su, J. Xia, and V.-T. Nguyen, "Adaptive fuzzy tracking control of flexible-joint robots with full-state constraints," *IEEE Transactions on Systems, Man, and Cybernetics: Systems*, vol. 49, no. 11, pp. 2201-2209, 2019.

[25] W. Sun, J.-W. Lin, S.-F. Su, N. Wang, and M. J. Er, "Reduced adaptive fuzzy decoupling control for lower limb exoskeleton," *IEEE Transactions on Cybernetics*, 2020. DOI: 10.1109/TCYB.2020.2972582

[26] S.-H. Wen, W. Zheng, S.-D. Jia, Z.-X. Ji, P.-C. Hao, and H.-K. Lam, "Unactuated force control of 5-DOF parallel robot based on fuzzy PI," *International Journal of Control Automation and Systems*, vol. 18, no. 6, pp. 1629-1641, 2020.

[27] J. W. Glasheen and T. A. McMahon, "Vertical water entry of disks at low froude numbers," *Physics of Fluids*, vol. 8, no. 8, pp. 2078-2083, 1996.

[28] C.-C. Lin, R.-C. Chen, and T.-L. Li, "Experimental determination of the hydrodynamic coefficients of an underwater manipulator," *Journal of Robotic Systems*, vol. 16, no. 6, pp. 329-338, 1999.

[29] S. S. Ge, C. C. Hang, T. H. Lee, and T. Zhang, *Stable Adaptive Neural Network Control*, Kluwer, Norwell, MA, 2001.

[30] J. Park and I. W. Sandberg, "Universal approximation using radial-basis-function networks," *Neural Computation*, vol. 3, no. 2, pp. 246-257, 1991.

Gyoung-Hahn Kim received his B.S. degree in mechanical engineering from Yeungnam University, Gyeongsan, Korea in 2013, and an M.S. degree in mechanical engineering at Pusan National University, Busan, Korea in 2019. He is currently a Researcher, Pusan National University, pursuing his Ph.D. degree. His research interests include sliding mode control, adaptive neural network control, reinforcement deep learning, control theory, and control applications to industrial robotics.

Phuong-Tung Pham received his B.S. and M.S. degrees in mechanical engineering from Ho Chi Minh City University of Technology, in 2016 and 2018, respectively. He is currently a Ph.D. candidate in the School of Mechanical Engineering, Pusan National University, Korea. His research interests include nonlinear control, adaptive control, vibration control, and control of distributed parameter systems.

Quang Hieu Ngo received his B.S. degree in mechanical engineering from Ho Chi Minh City University of Technology, Vietnam, in 2002, an M.S. degree in mechatronics from Asian Institute of Technology, Thailand, in 2007, and a Ph.D. degree in mechanical engineering from Pusan National University, Korea, in 2012. He is currently an Associate Professor in the Department of Mechanical Engineering, Can Tho University. His research interests include port automation, control of axially moving systems, sliding mode control, adaptive control, and input shaping control.

Quoc Chi Nguyen received his B.S. degree in mechanical engineering from Ho Chi Minh City University of Technology (HCMUT), Vietnam, in 2002, an M.S. degree in cybernetics from HCMUT, Vietnam, in 2006, and a Ph.D. degree in mechanical engineering from the Pusan National University, Korea, in 2012. Dr. Nguyen was a Marie Curie FP7 Postdoctoral Fellow at the School of Mechanical Engineering, Tel Aviv University, from 2013 to 2014. He is currently an Associate Professor with the Department of Mechatronics, HCMUT. Dr. Nguyen's current research interests include nonlinear systems theory, adaptive control, robotics, and distributed parameter systems.